Nuclear Engineering and Technology 50 (2018) 957–962

Contents lists available at ScienceDirect

Nuclear Engineering and Technology

journal homepage: www.elsevier.com/locate/net

Original Article

Investigation of gamma radiation shielding capability of two clay materials

S.F. Olukotun [a, *], S.T. Gbenu [b], F.I. Ibitoye [b], O.F. Oladejo [c], H.O. Shittu [d], M.K. Fasasi [b], F.A. Balogun [b]

[a] Department of Physics and Engineering Physics, Obafemi Awolowo University, Ile-Ife, Nigeria
[b] Centre for Energy Research and Development (CERD), Obafemi Awolowo University, Ile-Ife, Nigeria
[c] Department of Mathematical and Physical Science, Osun State University, Osogbo, Nigeria
[d] Department of Science Infrastructure, National Agency for Science and Engineering Infrastructure (NASENI), Abuja, Nigeria

ARTICLE INFO

Article history:
Received 22 February 2018
Received in revised form
7 May 2018
Accepted 8 May 2018
Available online 30 May 2018

Keywords:
Clay materials
WinXCom
Particle-induced X-ray emission (PIXE)
Gamma radiation shielding capability (GRSC)

ABSTRACT

The gamma radiation shielding capability (GRSC) of two clay-materials (Ball clay and Kaolin)of South-western Nigeria (7.49°N, 4.55°E) have been investigated by determine theoretically and experimentally the mass attenuation coefficient, μ/ρ (cm^2g^{-1}) of the clay materials at photon energies of 609.31, 1120.29, 1173.20, 1238.11, 1332.50 and 1764.49 keV emitted from ^{214}Bi ore and ^{60}Co point source. The mass attenuation coefficients were theoretically evaluated using the elemental compositions of the clay-materials obtained by Particle-Induced X-ray Emission (PIXE) elemental analysis technique as input data for WinXCom software. While gamma ray transmission experiment using Hyper Pure Germanium (HPGe) spectrometer detector to experimentally determine the mass attenuation coefficients, μ/ρ (cm^2g^{-1}) of the samples. The experimental results are in good agreement with the theoretical calculations of WinXCom software. Linear attenuation coefficient (μ), half value layer (HVL) and mean free path (MFP) were also evaluated using the obtained μ/ρ values for the investigated samples. The GRSC of the selected clay-materials have been compared with other studied shielding materials. The cognizance of various factors such as availability, thermo-chemical stability and water retaining ability by the clay-samples can be analyzed for efficacy of the material for their GRSC.

1. Introduction

Nigeria is considering nuclear technology as alternative source of energy to solve her erratic power problem [1]. Coupled with increasing use of radioactive isotopes and radiation emitting instruments in different fields, it is imperative to study GRSC of some readily available materials use for building such as clays.

Clay materials are used for construction and building purpose in many developed and developing nations. Clay products such as ceramic wares, burnt bricks, and tiles (for roofing and floor) are cheaper and more durable building materials than cement, especially under tropical condition [2].

That ionizing radiation can be injurious is beyond dispute, therefore, the principal function of a radiation shield is to attenuate the radiation emitted by a source to an acceptable level in the region beyond the shield, taking into account the hazard that may result from exposure to such ionizing radiation [3–5].

It has been discovered that clay possesses good refractory properties: High melting point, thermo-chemical stability, good mechanical strength at high temperature, high thermal shock resistance, low thermal shrinkage and high resistance to corrosion [6]. Interestingly, Clay is a composite material which is abundantly available thus proves to be eco-friendly, cost-effective and non-poisonous [7]. These properties make clay materials suitable for consideration for shielding purpose [8–12].

Among other kinds of ionizing radiation, gamma ray is proven to be the most difficult to shield [8–10]. The penetrating power of the gamma is due to the fact that it has no charge or mass. Gamma shielding is therefore more effectively performed by materials with high atomic mass number and high density [11].

The interaction of γ-ray depends on the incident photon energy. The linear attenuation coefficient, μ (cm^{-1}) is the most important

* Corresponding author.
E-mail addresses: olukotunsf@oauife.edu.ng, olukotunsf@yahoo.com (S.F. Olukotun).

https://doi.org/10.1016/j.net.2018.05.003

quantity characterizing the penetration and diffusion of gamma radiation in a medium. The linear attenuation coefficient, μ describes the fraction of a beam of gamma-rays that is absorbed or scattered per unit thickness of the absorber. The total linear attenuation coefficient μ for photons of a given energy in a given material is due to contributions from the various physical processes (majorly from photoelectric effect, Compton scattering, and Pair production) that can remove photons from the beam. The linear attenuation coefficient μ of a material depends on its density. The dependence of the linear attenuation coefficient μ on the absorber density, ρ is overcome by normalizing it with the absorber density. The mass attenuation coefficient (μ/ρ) is really of more fundamental value than the linear coefficient, because it does not depend on the actual density and physical state of the absorber.

Half Value Layer (HVL) and mean free path (MFP) are also important parameters to ascertain shielding capability of a material. Half Value Layer (HVL) is the thickness of a shielding material necessary to reduce the intensity of the gamma-ray to half its original; while the average distance a unit radiation can travel in a material without having any kind of interaction is called mean free path (MFP).

In recent years, several studies relevant to the measurement of mass attenuation coefficient, linear attenuation coefficient, Half Value Layer (HVL) and mean free path (MFP) for different types of composite materials have been published [13–28].

In this study GRSC for clay-materials found at Ile-Ife (Southwestern Nigeria) has been carried out. The mass attenuation coefficients of two clay materials being a naturally abound composite material with good refractory properties have been determined theoretically and experimentally to know their GRSC.

2. Theory

When a gamma-ray beam passes through a sample of thickness x (cm) under narrow beam geometry, the photons are transmitted according to Beer-Lambert's law [29,30].

$$I = I_o \exp(-\mu x) \tag{1}$$

where I_o and I are gamma-ray intensity before and after passing through a sample of thickness, x (cm) respectively, μ (cm^{-1}) is the linear attenuation coefficient of the sample.

The linear attenuation coefficient can be described in term of mass attenuation coefficient as follows:

$$\mu = \left(\mu/\rho\right)\rho = \mu_s\rho \tag{2}$$

where $\mu_s = \mu/\rho$ ($cm^2\ g^{-1}$) is the mass attenuation coefficient and ρ (g cm^{-3}) is the density of the sample. With Eq. (2), Eq. (1) can be rewritten as follows:

$$I = I_o \exp(-\mu_s d) \tag{3}$$

where d (g cm^{-2}) is the mass thickness of the sample.

Eq. (3) may be written in the following linear form:

$$In\ I = -\mu_s d + InI_o \tag{4}$$

For compound or mixture, the mass attenuation coefficient is the sum of separate contributions of each of the elements that made up the compound or the mixture. Hence an overall mass attenuation coefficient of compound or mixture can be written thus

$$\mu_s = \left(\frac{\mu}{\rho}\right)_{mix} = \sum_i \omega_i \left(\frac{\mu}{\rho}\right)_i \tag{5}$$

This expression is well known as **mixture rule** (also known as **Bragg law).**

ω_i is the fraction by weight of the element i which makes up the absorber and it express thus

$$\omega_i = \frac{a_i A_i}{\sum a_j A_j} \tag{6}$$

here A_i is the atomic mass of the i_{th} element, and α_i is the number of atoms of this element in the compound.

Half Value Layer (HVL) can be calculated using the following relation [20–23].

$$HVL = \frac{0.693}{\mu} \tag{7}$$

Meanwhile, mean free path (MFP) is reciprocal of total linear attenuation coefficient (μ).

3. Methodology

3.1. Preparation of the clay-materials and elemental analysis

Kaolin and Ball clay, the two types of clays, were collected from Government Reserve Forest, Ladugbo, Ile – Ife, Southwest Nigeria (7.49°N, 4.55°E), as-mined in lump form, crushed to suitable sizes and sun-dried. The samples were pulverized, sieved (with sieve of mesh sizes 2 μm), moulded and dried in accordance to American Society for Testing and Material (ASTM) standards [31]. Carbolite Muffled Furnace was used to bake the samples at temperatures 1000°C. Fig. 1 show Ball Clay samples labelled Sample A1 and A2 for the unbaked and those that were baked at 1000°C respectively, while B1 and B2 are Kaolin samples for the unbaked and those that were baked at 1000°C respectively. The samples were pelletized. To

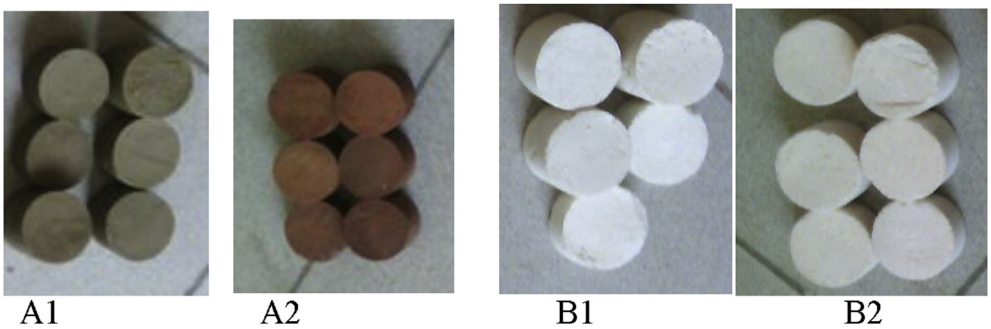

Fig. 1. Ball clay (A1: Unbaked; A2: Baked) and Kaolin (B1: Unbaked; B2: Baked).

determine elemental concentrations of the samples, Tandem Pelletron Accelerator (1.7 MV, Model 5SDH) was used for Particle Induced X-ray Emission (PIXE). The compositions have been listed in Table 1.

3.2. Theoretical mass attenuation coefficients of the samples

The parameter (i.e. μ/ρ) required for the analysis of GRSC of the samples has been evaluated with WinXcom software. WinXCom is a computer program and data base which can be used to calculate photon cross sections for scattering, photoelectric absorption and pair production, as well as total attenuation coefficients, in any element, compound or mixture, at energies from 1 keV to 100 GeV [32]. The input elemental compositions (PIXE results) of clay-samples were used. Computation is based on the Eqs. (5)–(6).

3.3. Experimental mass attenuation coefficients of the samples

Transmission experiment under a narrow geometrical condition at photon energies of 609.31, 1120.29, 1173.20, 1238.11, 1332.50 and 1764.49 keV emitted from ^{214}Bi ore and ^{60}Co point source were used to experimentally determine the attenuation coefficients of the samples. Bismuth is about twice as abundant as gold in the Earth's crust and the most important ores of bismuth are bismuthinite and bismite [33]. This geometric was achieved by the arrangement of lead collimator shields which enclosed HPGe semiconductor detector. The clay samples of various mass thickness d (g cm^{-2}) was placed in between the source and the detector (Fig. 2). The Hyper Pure Germanium (HPGe) gamma ray spectrometer at Centre for Energy Research and Development (CERD), Obafemi Awolowo University, Ile-Ife was used for the experimental work. From Eq. (4), mass attenuation coefficient μ_s (cm^{2}g^{-1}) was experimentally obtained from the measured values of (I_o/I) and d (g cm^{-2}).

4. Results and discussion

4.1. Elemental analysis

The PIXE elemental analysis result for ball clay and kaolin are shown in Table 1. The results show that the clay materials are majorly made up of silica, alumina plus appreciable concentration of iron, alkali and alkaline earth elements. Ball clay is majorly made up of 58% Silicon, 19% Aluminum, and 9% Iron; while Kaolin is 56% Silicon, 36% Aluminum and 7% Calcium as shown on Table 1. The results show that the concentration of Aluminum in Kaolin is twice that in Ball clay, while there is 9% of Ball clay is iron but it concentration is almost insignificant in Kaolin. However, there is 7% of Calcium in Kaolin and None in Ball clay. These results agreed with other published works [2,6].

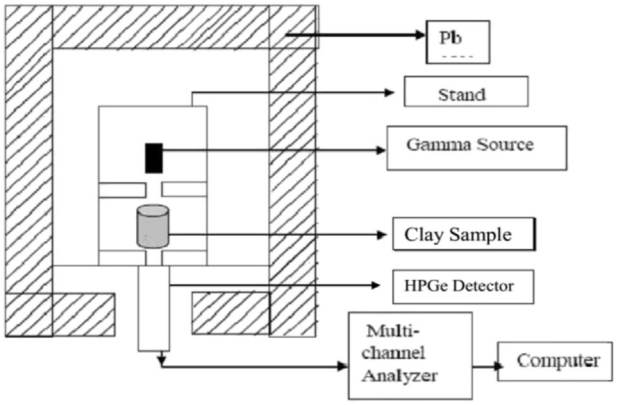

Fig. 2. Illustration of the experimental setup.

4.2. Mass attenuation coefficients, linear attenuation coefficient (μ), half value layer (HVL) and mean free path (MFP)

The theoretical and experimental mass attenuation coefficients of the samples at 609.31, 1120.29, 1173.20, 1238.11, 1332.50 and 1764.49 keV gamma energy for both ball clay and kaolin were obtained (Table 2). From the table it can be seen that mass attenuation coefficients of both samples decreases as energy increases [20–24,34]. The results also show that there is a good agreement between the theoretical and experimental values of mass attenuation coefficients of the clay materials.

Table 3 shows the theoretical and experimental linear attenuation coefficients (μ) of the samples and their variations with gamma ray energies. It is clear that all the samples have nearly same value at specified gamma energy. This is buttress by nearly same density values of the samples. It is observed that the μ values are influenced by chemical contents, photon energy and density.

Table 1
Elemental composition of the samples.

Element	Sample A1	Sample A2	Sample B1	Sample B2
	Density (gcm^{-3}) = 1.99	Density (gcm^{-3}) = 1.96	Density (gcm^{-3}) = 1.99	Density (gcm^{-3}) = 1.96
	Ele. Conc. By Wt.	Ele. Conc. By Wt.	Ele. Conc. By Wt.	Ele. Conc. By Wt.
Mg	1.44E-02	1.11E-02	0.00E+00	0.00E+00
Al	3.54E-01	2.08E-01	3.59E-01	3.61E-01
Si	5.59E-01	6.39E-01	5.52E-01	5.58E-01
P	0.00E+00	2.96E-02	0.00E+00	0.00E+00
Cl	6.40E-04	4.96E-03	7.04E-04	0.00E+00
K	1.74E-02	1.34E-02	6.68E-02	6.53E-02
Ca	2.70E-03	2.96E-04	2.79E-03	1.31E-03
Ti	8.58E-03	1.97E-04	5.12E-04	5.04E-04
V	1.56E-04	8.79E-04	0.00E+00	7.28E-05
Cr	9.88E-05	9.23E-02	4.76E-05	0.00E+00
Mn	4.58E-04	2.77E-05	1.68E-04	1.55E-04
Fe	4.18E-02	1.36E-04	1.68E-02	1.32E-02
Cu	1.51E-05	0.00E+00	0.00E+00	0.00E+00
Zn	5.73E-05	0.00E+00	1.26E-04	9.98E-05
Rb	1.05E-04	1.11E-03	6.32E-04	5.86E-04
Zr	4.56E-04	0.00E+00	0.00E+00	0.00E+00
Total	**1.0000**	**1.0000**	**1.0000**	**1.0000**

Table 2
Mass attenuation coefficients of the samples.

Energy (KeV)	Theoretical mass attenuation coefficient, μ_s (cm^2 g^{-1})				Experimental mass attenuation coefficient (cm^2 g^{-1})			
	A1	A2	B1	B2	A1	A2	B1	B2
609.31	0.0790	0.0788	0.0791	0.0791	0.0817 ± 0.0033	0.0817 ± 0.0033	0.0815 ± 0.0031	0.0817 ± 0.0031
1120.29	0.0592	0.0588	0.0592	0.0593	0.0613 ± 0.0031	0.0613 ± 0.0031	0.0612 ± 0.0030	0.0613 ± 0.0028
1173.20	0.0578	0.0575	0.0579	0.0579	0.0601 ± 0.0029	0.0600 ± 0.0029	0.0601 ± 0.0028	0.0602 ± 0.0028
1238.11	0.0563	0.0559	0.0563	0.0563	0.0578 ± 0.0030	0.0578 ± 0.0028	0.0578 ± 0.0027	0.0578 ± 0.0028
1332.50	0.0542	0.0539	0.0543	0.0543	0.0565 ± 0.0028	0.0564 ± 0.0027	0.0565 ± 0.0026	0.0564 ± 0.0027
1764.49	0.0470	0.0467	0.0470	0.0470	0.0494 ± 0.0028	0.0494 ± 0.0027	0.0493 ± 0.0026	0.0493 ± 0.0026

Table 3
Linear attenuation coefficient (μ) of the samples.

Energy (KeV)	Theoretical μ (cm^{-1})				Experimental μ (cm^{-1})			
	$A1_{TH}$	$A2_{TH}$	$B1_{TH}$	$B2_{TH}$	$A1_{EX}$	$A2_{EX}$	$B1_{EX}$	$B2_{EX}$
609.31	0.157	0.154	0.157	0.155	0.163	0.160	0.162	0.163
1120.29	0.118	0.115	0.118	0.116	0.122	0.120	0.122	0.122
1173.20	0.115	0.113	0.115	0.113	0.120	0.118	0.120	0.120
1238.11	0.112	0.110	0.112	0.110	0.115	0.113	0.115	0.115
1332.50	0.108	0.106	0.108	0.106	0.112	0.111	0.112	0.112
1764.49	0.094	0.092	0.094	0.092	0.098	0.097	0.098	0.098

Table 4
Half value layer (HVL) of the samples.

Energy (KeV)	Theoretical HVL (cm)				Experimental HVL (cm)			
	A1	A2	B1	B2	A1	A2	B1	B2
609.31	4.408	4.487	4.403	4.470	4.262	4.328	4.273	4.262
1120.29	5.882	6.013	5.882	5.962	5.681	5.768	5.690	5.681
1173.20	6.025	6.149	6.015	6.107	5.794	5.893	5.794	5.785
1238.11	6.185	6.325	6.185	6.280	6.025	6.117	6.025	6.025
1332.50	6.425	6.560	6.413	6.511	6.164	6.269	6.164	6.174
1764.49	7.409	7.571	7.409	7.523	7.049	7.157	7.064	7.064

HVL and MFP are important parameters that reflect the fact that energetic photons have the capability to penetrate a sample with the increment of photon energy. The HVL and MFP were evaluated from the theoretical and experimental mass attenuation coefficient values obtained. The results are listed in Tables 4 and 5 respectively. From Tables 4 and 5, it can be observed that the values of HVL and MFP increase with an increase in photon energy for all the samples. It has to be noted that at each specified gamma energies, HVL and MFP values are nearly the same for all the samples.

4.3. Comparison of GRSC of the clay materials with studied shielding materials

In order to ascertain the effectiveness of the samples under investigation, the obtained values of mass attenuation coefficient, μ, HVL and MFP were compared with that of ordinary, hematite-serpentine, ilmenite-limonite, basalt-magnetite, Ilmenite, Steel Scrap, and Steel-magnetite concretes [35] at 1170 and 1330 keV as shown in Table 6. It is obvious that these parameters are density and photon energy dependent [20–25,35]. The densities values of the samples under investigation are nearly the same (1.96–1.99 g/cm^3) and are lower, thus it is evident that the HVL and MFP values

Table 5
Mean free path (MFP) of the samples.

Energy (KeV)	Theoretical MFP (cm)				Experimental MFP (cm)			
	A1	A2	B1	B2	A1	A2	B1	B2
609.31	6.361	6.475	6.353	6.450	6.151	6.245	6.166	6.151
1120.29	8.488	8.677	8.488	8.604	8.198	8.323	8.211	8.198
1173.20	8.694	8.873	8.679	8.812	8.361	8.503	8.361	8.347
1238.11	8.926	9.127	8.926	9.062	8.694	8.827	8.694	8.694
1332.50	9.271	9.466	9.254	9.396	8.894	9.046	8.894	8.910
1764.49	10.692	10.925	10.692	10.855	10.172	10.328	10.193	10.193

Table 6
Comparison of GRSC of the clay materials with studied shielding materials.

Samples		Density (gcm^{-3})	1173.20 keV				1332.50 keV			
			[a]MAC (cm^2g^{-1})	μ (cm^{-1})	HVL (cm)	MFP (cm)	[a]MAC (cm^2g^{-1})	μ (cm^{-1})	HVL (cm)	MFP (cm)
[35]	Ordinary-concrete	2.30	0.0594	0.1366	5.0725	7.3196	0.0556	0.1279	5.4191	7.8198
	Hematite-serpentine	2.50	0.0585	0.1463	4.7385	6.8376	0.0548	0.1370	5.0584	7.2993
	Ilmenite-limonite	2.90	0.0572	0.1659	4.1777	6.0285	0.0536	0.1554	4.4583	6.4334
	Basalt-magnetite	3.05	0.0583	0.1778	3.8973	5.6238	0.0546	0.1665	4.1614	6.0049
	Ilmenite	3.50	0.0571	0.1999	3.4676	5.0038	0.0535	0.1873	3.7009	5.3405
	Steel Scrap	4.00	0.0571	0.2284	3.0342	4.3783	0.0535	0.2140	3.2383	4.6729
	Steel-magnetite	5.11	0.0565	0.2887	2.4003	3.4636	0.0529	0.2703	2.5636	3.6993
This work	A1	1.99	0.0601	0.1196	5.7944	8.3613	0.0565	0.1124	6.1636	8.8940
	A2	1.96	0.0600	0.1176	5.8929	8.5034	0.0564	0.1105	6.2690	9.0462
	B1	1.99	0.0601	0.1196	5.7944	8.3613	0.0565	0.1124	6.1636	8.8940
	B2	1.96	0.0602	0.1180	5.8733	8.4752	0.0564	0.1105	6.2690	9.0462

[a] MAC is the mass attenuation coefficient.

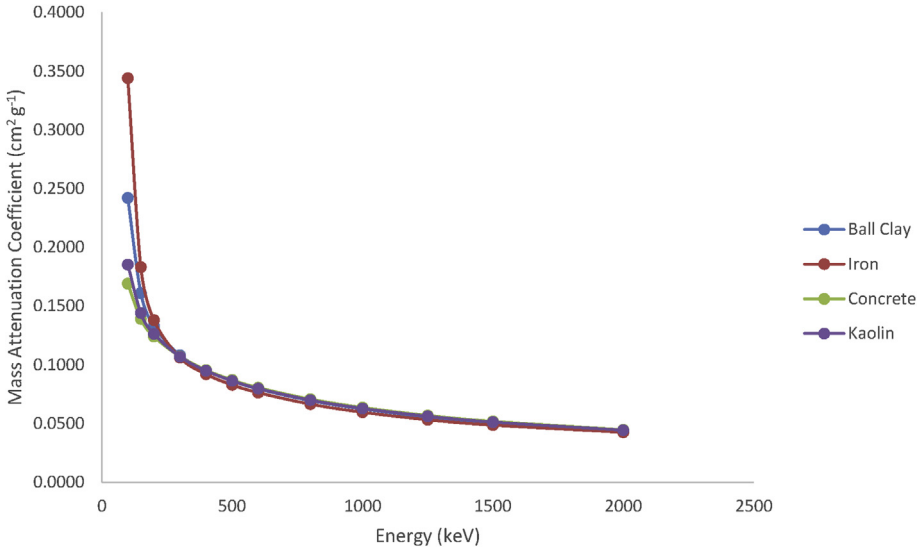

Fig. 3. Comparison of GRSC of the clay materials with iron and concrete.

of the samples under study are close only to that of ordinary concrete. More also, the mass attenuation coefficients of the clay materials were compared with values of known shielding materials (concrete and iron) between 100 to 2000 KeV gamma photon energies [36]. Ball clay is better than ordinary concrete at low incident photon energy where photoelectric absorption is the dominant interaction process (Fig. 3). The photoelectric process is the predominant mode of interaction for gamma rays of relatively low energy. The process is enhanced for absorber materials of high atomic number Z or effective atomic number Z_{eff} for a multiple element compound or mixture [8]. The cognizance of various factors such as cost, availability, thermo-chemical stability and water retaining ability by the clay-samples might be an advantage of utilizing the clay materials in engineering structures and building construction to shield gamma-rays.

5. Conclusion

GRSC of Ball clay and Kaolin were experimentally and theoretically examined. The results of the experimentally determined attenuation coefficient agree with the theoretically evaluated values. The obtained values of mass attenuation coefficient, μ, HVL and MFP were compared with values of different types of studied shielding materials. Considering factors such as availability, cost, thermo-chemical stability and energy range of 100–2000 KeV, we can conclude that clay materials can be a choice for gamma radiation shielding for both medical and nuclear applications.

Acknowledgement

We will like to register our deep sense of appreciation to the entire staff of Centre for Energy Research and Development (CERD), Obafemi Awolowo University, Ile-Ife for their help during measurements. We wish also to uniquely thank Dr. B. Aremo of Department of Material Science and Engineering, and Dr. F. S. Olise of Department of Physics and Engineering Physics, Obafemi Awolowo University, Ile-Ife for their guide at various point of the work.

References

[1] https://www.vanguardngr.com/2017/11/nigeria-signs-pact-russia-nuclear-energy/.
[2] E. Nnuka, C. Enejor, Characterisation of Nahuta clay for industrial and commercial applications, Niger. J. Eng. Mater. 2 (2001) 9–12.
[3] E.J. Hall, Radiobiology for the Radiologist, fifth ed., Lippincott Williams & Wilkins, New Yoke, Philadephia, 2000.
[4] J.E. Turner, Atoms, Radiation and Radiation Protection, third ed., John Wiley and Sons, New York, 2007.
[5] G.F. Knoll, Radiation Detection and Measurement, third ed., John Wiley and Sons, New York, 2000.
[6] J.A. Omotoyinbo, Working properties of some selected refractory clay deposits in southwestern Nigeria, J. Miner. Mater. Charact. Eng. 7 (2008) 233–245.
[7] O.S. Adegoke, Guide to the Non-metal Mineral Industrial Potential of Nigeria, Raw Materials Research and Development Council, Kaduna, Nigeria, 1980, pp. 110–120. RMRDC.
[8] R.D. Evans, The Atom Nucleus, in: THM (Ed.), McGraw-Hill, New York, 1995.
[9] E.P. Miller, Radiation Attenuation Characteristics of Structural Concrete, OAK Ridge National Laboratory, Tennessee, 1958.
[10] E. Yilmaz, et al., Gamma ray and neutron-shielding properties of some concrete materials, Ann. Nucl. Energy 38 (2011) 2204–2212.
[11] N.A. Alallak, Factors affecting gamma ray transmission, Jordan J. Phys. 5 (2012) 77–88.
[12] Oak ridge national laboratory, Early test facilities and analytic methods. Special Session Radiation Protection and Shielding, US, Department of energy, Chicago, 1992, pp. 1–8.
[13] H.M. Soylu, et al., Gamma radiation shielding efficiency of a new lead-free composite material, J. Radioanal. Nucl. Chem. 305 (2015) 529–534.
[14] I. Akkurt, et al., Chemical corrosion on gamma-ray attenuation properties of barite concrete, J. Saudi Chem. Soc. (2012) 199–202.
[15] S.M. Harjinder, Experimental investigation of clay fly-ash bricks for gamma-ray shielding, Nucl. Eng. Technol. 48 (2016) 1230–1236.
[16] M.E. Medhat, Gamma-ray attenuation coefficients of some building materials in Egypt, Ann. Nucl. Energy 36 (2009) 849–852.
[17] B. Oto, A. Gur, Gamma-ray shielding of concretes including magnetite in different rate, Int. J. Phys. Sci. 8 (2013) 310–314.
[18] B. Oto, et al., Photon attenuation properties of some concretes containing barite and colemanite in different rates, Ann. Nucl. Energy 51 (2013) 120–124.
[19] S.O. Shamsan, et al., Attenuation coefficients and exposure buildup factor of some rocks for gamma ray shielding applications, Radiat. Phys. Chem. 148 (2018) 86–94.
[20] M.I. Sayyed, et al., Determination of nuclear radiation shielding properties of some tellurite glass using MCNP5 code, Radiat. Phys. Chem. 150 (2018) 1–8.
[21] A.H. Taqi, H.J. Khalil, Experimental and theoretical investigation of gamma attenuation of building materials, J. Nucl. Particle Phys. 7 (1) (2017) 6–13.
[22] M.I. Sayyed, H. Elhouichet, Variation of energy absorption and exposure buildup factors with incident photon energy and penetration depth for borotellurite (B2O3-TeO2) glasses, Radiat. Phys. Chem. 130 (2017) 335–342.
[23] M.I. Sayyed, et al., Investigation of radiation shielding properties for MeO-PbCl2-TeO2 (MeO = Bi2O3, MoO3, Sb2O3, WO3, ZnO) glasses, Radiat. Phys. Chem. 144 (2018) 419–425.
[24] M.I. Sayyed, S.I. Qashou, Z.Y. Khattari, Radiation shielding competence of newly developed TeO2-WO3 glasses, J. Alloys Comp. 696 (2017) 632–638.
[25] H.O. Tekin, et al., Photon shielding characterizations of bismuth modified borate-silicate-tellurite glasses using MCNPX Monte Carlo code, J. Mater. Chem. Phys. 211 (2018) 9–16.
[26] M.I. Sayyed, G. Lakshminarayana, Structural, thermal, optical features and shielding parameters investigations of optical glasses for gamma radiation

shielding and defense applications, J. Non-Crystalline Solids 487 (2018) 53–59.
[27] M.G. Dong, et al., Investigation of gamma radiation shielding properties of lithium zinc bismuth borate glasses using XCOM program and MCNP5 code, J. Non-Crystalline Solids 468 (2017) 12–16.
[28] M. Kurudirek, et al., Effect of Bi_2O_3 on gamma ray shielding and structural properties of borosilicate glasses recycled from high pressure sodium lamp glass, J. Non-Crystalline Solids 745 (2017) 355–364.
[29] D. McAlister, Gamma Ray Attenuation Properties of Common Shielding Materials, University Lane Lisle, USA, 2012.
[30] M.E. Medhat, Application of gamma-ray transmission method for study, Ann. Nucl. Energy (2012) 53–59.
[31] S.A. Agbalajobi, Analysis on some physical and chemical properties of Oreke dolomite deposit, J. Miner. Mater. Charact. Eng. 4 (2013) 33–38.
[32] L.E. Gerward, WinXCom – a program for calculating X-ray attenuation coefficients, Radiat. Phys. Chem. 653–654 (2004).
[33] C.R. Hammond, The elements, in: Handbook of Chemistry and Physics, 81st ed., CRC Press, Boca Raton (FL, US), 2004, p. 4–1. ISBN 0-8493-0485-7.
[34] I.O. Olarinoye, Variation of effective atomic numbers of some thermoluminescence and phantom materials with photon energies, Res. J. Chem. Sci. (2011) 64–69.
[35] I.I. Bashter, Calculation of radiation attenuation coefficients for shielding concretes, Ann. Nucl. Energy 24 (1997) 1389–1401.
[36] J.R. Lamarsh, Introduction to Nuclear Engineering, Prentice Hall, New Jersey, 2001.